

Limits on single- and multinucleon decays in ^{127}I by inclusive measurements of nuclear γ and x rays

R. Hazama,¹ H. Ejiri,^{1,2} K. Fushimi,¹ and H. Ohsumi¹

¹Department of Physics, Osaka University, Toyonaka, Osaka 560, Japan

²Research Center for Nuclear Physics, Osaka University, Ibaraki, Osaka 567, Japan

(Received 20 December 1993)

Baryon-number-violating nucleon decays were studied by searching for x and γ rays associated with radioactive residual nuclei produced by single- and multinucleon decays in ^{127}I . Large volume NaI (Tl) detectors were used for the study. New lower limits of $\tau(n) > 4.7 \times 10^{24}$ yr and $\tau(p) > 3.0 \times 10^{24}$ yr were obtained on the mode-independent mean lives for the neutron and proton decays in ^{127}I , respectively. Lower limits of $\tau(nn) > 2.1 \times 10^{24}$ yr, $\tau(nnn) > 1.8 \times 10^{23}$ yr, and $\tau(nnnn) > 1.4 \times 10^{23}$ yr were deduced for the first time on the mode-independent mean lives for dineutron, trineutron, and tetraneutron decays in ^{127}I , respectively.

PACS number(s): 13.30.-a, 23.40.-s, 29.30.Kv

I. INTRODUCTION

Nucleon decay modes such as $p \rightarrow e^+\pi^0$, $p \rightarrow \bar{\nu}K^+$, $n \rightarrow \bar{\nu}K^0, \dots$ are predicted by grand unified theories (GUT's) [1,2]. These decay modes have been extensively studied by IMB, Kamioka, and Fréjus experiments [3-7] and references therein. The observed mean-life limit of $\tau(p \rightarrow e^+\pi^0) > 5.5 \times 10^{32}$ yr rules out minimal SU(5) model which predicted $\tau(p \rightarrow e^+\pi^0) \sim 3 \times 10^{31}$ yr [8]. It is very interesting to study various decay modes to test possible new classes of baryon-number-violating processes. ($B - L$)-violating nucleon decays and dinucleon decays of nucleons bound in nuclei are proposed as the possible new modes beyond the simplest SU(5) [9].

The experiments referred above are sensitive only to decay modes in which energetic charged particles are produced. They are not sensitive to invisible decay modes such as $n \rightarrow 3\nu$. It is very important to carry out inclusive measurements for nucleon decays, which are in-

sensitive to the decay modes. Mode-independent nucleon decays can be studied by searching for possible γ and x rays associated with radioactive residual nuclei produced by the nucleon decay in nuclei [10,11]. This method is useful for decay modes where direct measurement of the decay products are hard.

We studied the disappearance of nucleon(s) from ^{127}I in the NaI(Tl) scintillator itself. A neutron hole is produced in ^{126}I in case of the neutron disappearance in ^{127}I , while a proton hole in ^{126}Te in case of the proton disappearance. In case that these hole states are located above the neutron threshold, they deexcite promptly by emitting neutron(s), and γ rays if excited states are populated after neutron emission(s). Deexcitation modes of neutron-hole states in ^{126}I and those of proton-hole states in ^{126}Te are shown in Fig. 1. Note that the proton emission is suppressed by a large Coulomb barrier. After the prompt deexcitations, ground states and metastable (isomeric) states in residual nuclei decay mostly by elec-

TABLE I. Identification modes of nucleon disappearance and lower limits on the nucleon lifetime. For each mode, decay modes to be measured Mode, identification modes ID, sum energies to be measured in the NaI(Tl) detector $E(\text{sum})$, the effective number of decaying nucleons in a simple shell model m , the upper limit on the counting rate per day at 90% C.L. Y_{max} , and the lower limit on nucleon lifetime at 90% C.L. (68% C.L.) τ_{min} are given.

Mode	ID	$E(\text{sum})$ (keV)	m	Y_{max} (counts/day)	τ_{min} (10^{24} yr)
$n \rightarrow x$	$^{126}\text{I} \rightarrow ^{126}\text{Te}(2^+)$	699	34	39.4	1.1(3.3)
	$^{126}\text{I} \rightarrow ^{126}\text{Te}(\text{g.s.})$	33.2	34	36.0	1.5(2.4)
	$^{125}\text{I} \rightarrow ^{125}\text{Te}(\frac{3}{2}^+)$	68.7	22	39.7	4.7(9.6)
	$^{124}\text{I} \rightarrow ^{124}\text{Te}(2^+)$	636	16	67.0	0.26(0.42)
	$^{124}\text{I} \rightarrow ^{124}\text{Te}(\text{g.s.})$	33.2	16	36.0	0.94(1.5)
	$^{123}\text{I} \rightarrow ^{123}\text{Te}(\frac{3}{2}^+)$	192	2	54.4	0.28(0.59)
	$^{122}\text{I} \rightarrow ^{122}\text{Te}(2^+)$	597	1	67.6	0.0022(0.0036)
	$^{122}\text{I} \rightarrow ^{122}\text{Te}(\text{g.s.})$	33.2	1	36.0	0.045(0.070)
$p \rightarrow x$	$^{125}\text{Te}(\frac{11}{2}^-) \rightarrow ^{125}\text{Te}(\text{g.s.})$	145	20	54.4	3.0(6.3)
	$^{123}\text{Te}(\frac{11}{2}^-) \rightarrow ^{123}\text{Te}(\text{g.s.})$	247.5	8	88.8	0.65(1.0)

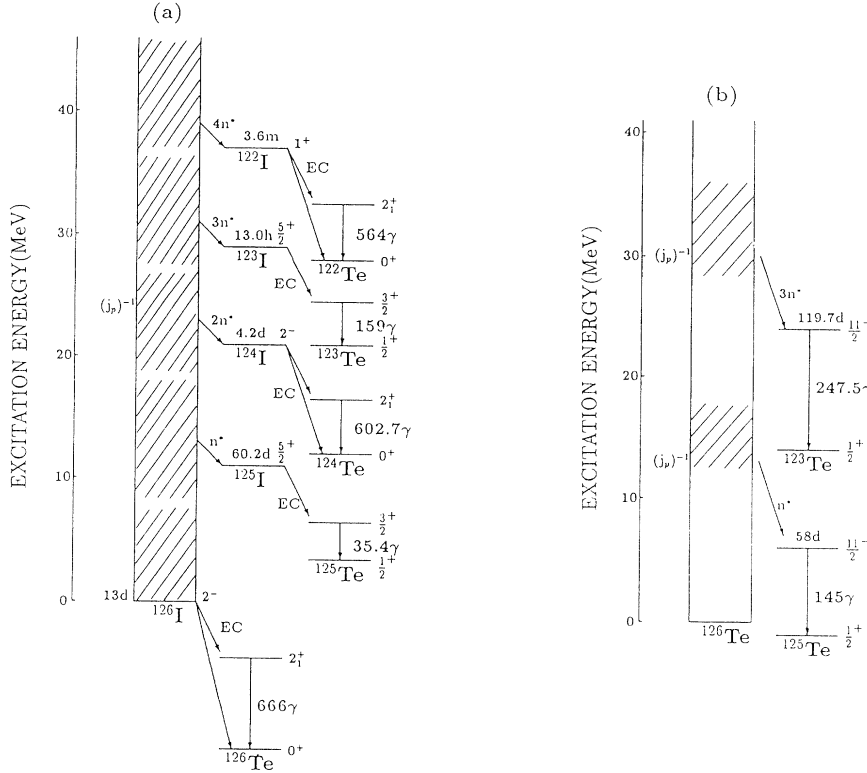


FIG. 1. Deexcitation modes of neutron-hole states in ^{126}I (a) and proton-hole states in ^{126}Te (b). n^* denotes neutrons emitted from these highly excited states. Decay schemes of EC and γ decay of residual nuclei after neutron evaporation are also displayed.

neutron capture (EC) to the ground and/or excited states in daughter nuclei as shown in Fig. 1. EC's are mostly followed by K x rays, since EC's in these medium-heavy nuclei are mainly of the K -electron capture process. If excited states are populated by EC, they deexcite by emitting γ rays, as shown in Fig. 1.

In the present work we measured the x rays and the γ rays, which follow EC of residual nuclei produced by the nucleon disappearance. Since EC is due to the weak interaction, it is a very slow process of the order of 10^2 – 10^6 sec. Thus the x rays and the γ rays following EC are well separated in time from all the prompt decay products and from all the prompt deexciting particles and γ rays. Consequently a single discrete line spectrum is expected at either $E = B_k$ or $E = B_k + E_x$, depending on whether EC feeds the ground state or the excited state. Here B_k and E_x stand for the binding energy of the K electron and the excitation energy of the excited state, respectively. They are listed in Table I. It is noted that all signals from the successive K, L, \dots x rays and γ rays are summed up in the present large volume NaI.

II. EXPERIMENTAL METHODS AND RESULTS

The search for nucleon disappearance has been carried out by using large NaI(Tl) scintillators in ELEGANTS V, which has been used for $\beta\beta$ decay experiments. Details of the NaI(Tl) detector and ELEGANTS V are given elsewhere [12–14]. The total mass of the NaI(Tl) is 770 kg, thus 2.29×10^{29} (1.64×10^{29}) neutrons (protons) in iodine nuclei in the detector are available for the study

of nucleon decays. The energy spectrum was measured for the live time of 179.5 days. The spectrum was also measured for the live time of 75.8 days at a lower discriminator setting in order to search for the x rays and low-energy γ rays.

The measured energy spectrum of the NaI(Tl) with live time of 179.5 days is shown in Fig. 2. It shows no prominent γ -ray peaks besides weak γ lines from known radioactive impurities. The major peaks seen in this spectrum are discussed in detail in Ref. [14]. In order to search for signals from nucleon disappearance, the following four energy regions were analyzed in detail. In the following analyses the measured energy resolutions of the detector are used for the widths of the Gaussian peaks. Typical energy resolution for the ^{214}Bi 609 keV γ ray is about $\Delta E/E = 9.8\%$ (FWHM).

(a) 400 keV–900 keV [Fig. 3(a)]. The spectrum is well reproduced in terms of the three Gaussian peaks of 609 keV (^{214}Bi), 768 keV (^{214}Bi), and 511 keV (positron annihilation) γ rays and a continuum component with third order polynomial functions, as shown in Fig. 3(a). The upper limits on the peak yields of the present concerns (699 keV, 636 keV, 597 keV) are listed in Table I.

(b) 200 keV–450 keV [Fig. 3(b)]. The spectrum is well reproduced in terms of the three Gaussian peaks of 242 keV, 295 keV, 352 keV γ rays of ^{214}Pb and a continuum component with third order polynomial functions, as shown in Fig. 3(b). The upper limit on the yield of the 247.5 keV peak is listed in Table I.

(c) 80 keV–250 keV [Fig. 3(c)]. The spectrum is well reproduced in terms of a broad Gaussian peak due to the K x rays of U-chain and Th-chain isotopes with energies

NaI Energy Spectrum

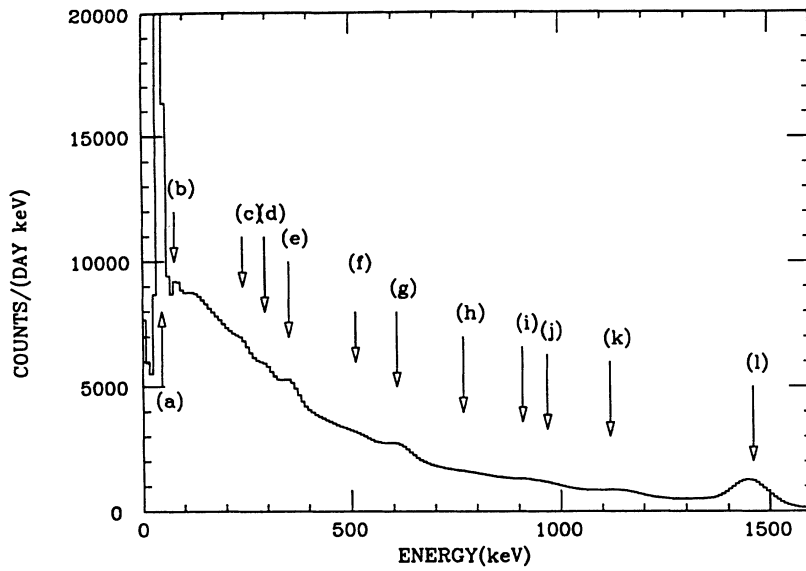


FIG. 2. The energy spectrum measured by the NaI detectors. The major background peaks are identified as follows: (a) 46.5 keV ^{210}Pb , (b) 77 keV U-chain x ray, (c) 242 keV ^{214}Pb , (d) 295 keV ^{214}Pb , (e) 352 keV ^{214}Pb , (f) 511 keV, (g) 609 keV ^{214}Bi , (h) 768 keV ^{214}Bi , (i) 911 keV ^{228}Ac , (j) 969 keV ^{228}Ac , (k) 1120 keV ^{214}Bi , and (l) 1461 keV ^{40}K .

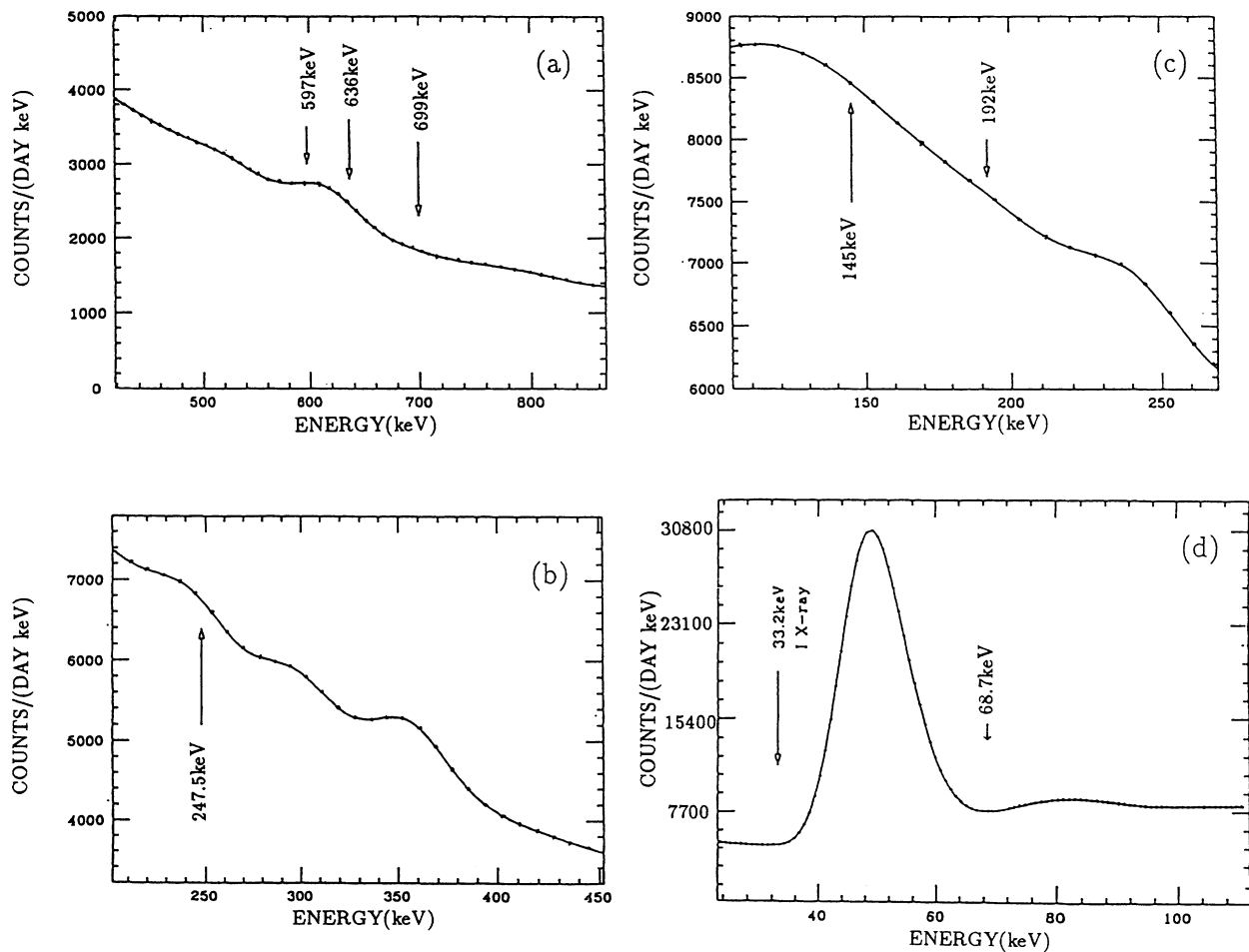


FIG. 3. The measured energy spectrum of NaI(Tl). Solid lines show the best fits with Gaussians of known peaks and third order polynomial functions of continuum component. The statistical errors are much smaller than the points.

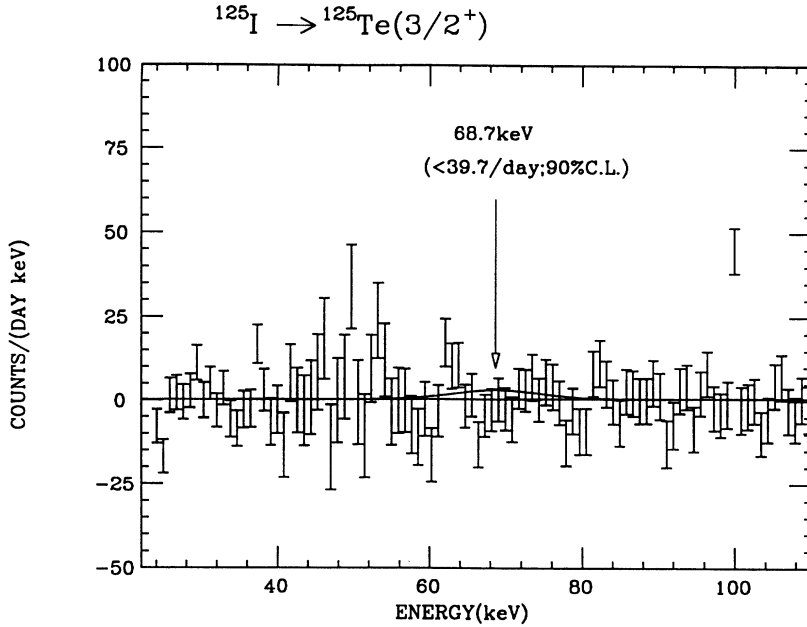


FIG. 4. An example of the energy spectrum after subtraction of the best fit function. This shows the same energy region as Fig. 3(d). The possible γ -ray peak, corresponding to 90% C.L., is drawn as a solid line.

around 80 keV, a Gaussian peak of the 242 keV γ ray of ^{214}Pb , and a continuum component with third order polynomial functions, as shown in Fig. 3(c). The upper limits on the yields of the 145 keV and 192 keV peaks are listed in Table I.

(d) 20 keV–120 keV [Fig. 3(d)]. The major background peak around 46.5 keV is caused by the β decay of ^{210}Pb . This peak has a tail at the higher energy side because the low energy β rays from ^{210}Pb are added to the 46.5 keV γ -ray peak. The spectrum is well reproduced in terms of the 46.5 keV peak with the β -ray tail, the K x rays around 80 keV, and a continuum component with third order polynomial functions, as shown in Fig. 3(d). The upper limits on the yields of the 68.7 keV and 33.2 keV peaks are obtained as listed in Table I. Typical energy spectrum after subtraction of the best fit function is shown in Fig. 4 as an example.

III. SINGLE-NUCLEON DECAYS

The effective number of nucleons in ^{127}I , which contribute to the nucleon decays of the present concern, is evaluated as follows. A hole is produced in ^{126}I (^{126}Te) after one neutron (proton) disappearance of ^{127}I . Deexcitation process of the hole state depends on the excitation energy (E_{ex}) of the state. The excitation energy (E_{ex}) is given by the difference between the binding energy of the decaying (disappearing) nucleon (E_b) and that of the least bound nucleon (E_s) in ^{127}I . Let us consider a case that the excitation energy is in the region of $\bar{E}_{\text{th}}^k < E_{\text{ex}} < \bar{E}_{\text{th}}^{k+1}$ ($k = 0, 1, 2, \dots$), where \bar{E}_{th}^k is the effective threshold energy of the k neutron evaporation (see Fig. 1). In this case the excited nucleus deexcites mainly by evaporating k neutrons. The effective threshold energy \bar{E}_{th}^k is approximately given by $\bar{E}_{\text{th}}^k = B_{\text{th}}^k + k\bar{E}_n^k$ where B_{th}^k are the threshold energies for emitting the k neutrons and \bar{E}_n^k is their average neutron kinetic energy.

Here \bar{E}_n^k is estimated on the basis of a statistical model. The proton evaporation modes are almost forbidden because of the large Coulomb barrier.

If a nucleon with the binding energy E_b between $\bar{E}_{\text{th}}^k + E_s$ and $\bar{E}_{\text{th}}^{k+1} + E_s$ ($k = 0, 1, 2, \dots$) decays, the hole state with the excitation energy of $\bar{E}_{\text{th}}^k < E_{\text{ex}} < \bar{E}_{\text{th}}^{k+1}$ is produced. Then it deexcites by evaporating k neutrons. Consequently the residual nucleus of $^{126-k}\text{I}$ is left in case of a neutron decay and $^{126-k}\text{Te}$ in case of a proton decay. In other words decaying neutrons (protons) in the energy interval of $\bar{E}_{\text{th}}^k + E_s < E_b < \bar{E}_{\text{th}}^{k+1} + E_s$ are relevant to EC of $^{126-k}\text{I}$ ($^{126-k}\text{Te}$) (see Table I). The number of the nucleons in that energy interval is evaluated by using a simple shell model. Binding energies of single-particle orbits in the nuclear potential were used [15]. The evaluated effective numbers of nucleons are summarized in Table I.

In this study we have analyzed 10 deexcitation modes of one nucleon-hole after nucleon decays in a nucleus. Among them 8 modes are caused by the neutron decay and 2 modes by the proton decay. The deduced lifetime limit τ of the nucleon decays is

$$\tau > N_n \frac{m}{N} b \frac{\varepsilon}{Y_{\text{max}}}, \quad (1)$$

where N_n is the number of neutrons or protons in the ^{127}I within the volume of 770 kg, m is the effective number of neutrons or protons, N is 74 and 53 for neutron and proton, respectively, b is the branching ratio of the γ or K x-ray emission after EC, ε is the peak efficiency of the γ and/or x ray, and Y_{max} is the upper limit on the counting rate. The efficiencies are determined by means of Monte Carlo methods. We used the GEANT3 Monte Carlo code [16] including a full description of the NaI detector. A simple shell model picture of the ^{127}I nucleus is used to obtain m as already discussed above. Using these values, the obtained lower limit on mean life

TABLE II. Identification modes of multinucleon disappearance and lower limits on the multinucleon lifetime. For each mode, decay modes to be measured Mode, identification modes ID, sum energies to be measured in the NaI(Tl) detector $E(\text{sum})$, the effective number of decaying nucleons in a simple shell model m , the upper limit on the counting rate per day at 90% C.L. Y_{max} , and the lower limit on multinucleon lifetime at 90% C.L. (68% C.L.) τ_{min} is given.

Mode	ID	$E(\text{sum})$ (keV)	m	Y_{max} (counts/day)	τ_{min} (10^{24} yr)
$nn \rightarrow x$	$^{125}\text{I} \rightarrow ^{125}\text{Te}(\frac{3}{2}^+)$	68.7	10	39.7	2.1(4.4)
	$^{124}\text{I} \rightarrow ^{124}\text{Te}(2^+)$	636	6	67.0	0.099(0.16)
	$^{124}\text{I} \rightarrow ^{124}\text{Te}(\text{g.s.})$	33.2	6	36.0	0.35(0.56)
	$^{123}\text{I} \rightarrow ^{123}\text{Te}(\frac{3}{2}^+)$	192	3	54.4	0.42(0.88)
$nnn \rightarrow x$	$^{124}\text{I} \rightarrow ^{124}\text{Te}(2^+)$	636	3	67.0	0.049(0.080)
	$^{124}\text{I} \rightarrow ^{124}\text{Te}(\text{g.s.})$	33.2	3	36.0	0.18(0.28)
	$^{123}\text{I} \rightarrow ^{123}\text{Te}(\frac{3}{2}^+)$	192	1	54.4	0.14(0.29)
$nnnn \rightarrow x$	$^{123}\text{I} \rightarrow ^{123}\text{Te}(\frac{3}{2}^+)$	192	1	54.4	0.14(0.29)

is as shown in Table I. The most stringent lower limit for the proton and neutron decays are obtained as $\tau(n) > 4.7 \times 10^{24}$ yr, $\tau(p) > 3.0 \times 10^{24}$ yr (90% C.L.).

IV. MULTINUCLEON DECAYS

By using the result obtained here we can obtain the new limits on mode-independent multinucleon decays such as $2N \rightarrow X$ (dinucleon decay), $3N \rightarrow X$ (trinucleon decay), and so on. For example, the process of $^{127}\text{I} \rightarrow ^{125}\text{I} + X + n + \gamma$, which is a one neutron disappearance followed by a one neutron evaporation, can be regarded as a two neutron decay (disappearance) of $^{127}\text{I} \rightarrow ^{125}\text{I} + X + \gamma$. A similar argument can be applied for the other multinucleon decays (disappearance). To estimate the number of possible combinations of decaying

nucleons, only neutrons in the same shell orbit are considered. In the case of the neutron-filled j orbit, the number of neutron pairs for the $2n$ decay is $m(2n, j) = \frac{1}{2}(2j+1)$, that for the $3n$ decay is $m(3n, j) = \frac{1}{3}(2j+1)$, and so on. We adopt the most conservative number of possible combinations of multinucleon disappearance, as listed in Table II, by using the similar consideration of a one nucleon disappearance. The most stringent lower limit for the multineutron disappearance is obtained as $\tau(nn) > 2.1 \times 10^{24}$ yr, $\tau(nnn) > 1.8 \times 10^{23}$ yr, $\tau(nnnn) > 1.4 \times 10^{23}$ yr (90% C.L.).

Our measured limits on nucleon decays are summarized in Table III compared with the other measurements. ^{130}Te (target) result is deduced from the geochemical data on xenon isotopes measured in old telluride ores [17]. Earth (target) results are indirectly measured for $n \rightarrow 3\nu_\mu$, $nn \rightarrow \nu_\mu \bar{\nu}_\mu, \dots$, modes by the CWI group

TABLE III. Lower limits (τ_{min}) on nucleon lifetime and multinucleon lifetime. The values, with 90% C.L., are given in units of 10^{25} yr. a: Ref. [17], obtained by measuring residual nuclei. These limits are deduced from the limit of 1.6×10^{25} yr by multiplying the proton and neutron ratio of $\frac{24}{52}$ and $\frac{28}{52}$, respectively. b: Ref. [18], deduced from the ν_μ flux observed by liquid scintillation detectors and flush tubes. c: Ref. [19], deduced from the neutrino flux observed by tracking calorimeter (iron); Fréjus experiment. d: Ref. [20], obtained by measuring high energy γ ray from the deexcitation of neutron-hole state; KAMIOKANDE experiment.

Decay target	Mode	Method	τ_{min} (10^{25} yr)	Comment
^{130}Te	$p \rightarrow x$ inclusive	Geochemical	0.74	a
	$n \rightarrow x$ inclusive	Geochemical	0.86	a
Earth	$n \rightarrow 3\nu_\mu$	Indirect	50	b
	$n \rightarrow \nu_e \nu_e \bar{\nu}_e$	Indirect	3	c
	$n \rightarrow \nu_\mu \nu_\mu \bar{\nu}_\mu$	Indirect	12	c
^{16}O	$n \rightarrow x$ inclusive	Direct	49	d
	^{127}I			
^{127}I	$p \rightarrow x$ inclusive	Direct	0.30	Present
	$n \rightarrow x$ inclusive	Direct	0.47	Present
Earth	$nn \rightarrow \nu_e \bar{\nu}_e$	Indirect	1.2	c
	$nn \rightarrow \nu_\mu \bar{\nu}_\mu$	Indirect	0.6	c
^{127}I	$nn \rightarrow x$ inclusive	Direct	0.21	Present
	$nnn \rightarrow x$ inclusive	Direct	0.018	Present
	$nnnn \rightarrow x$ inclusive	Direct	0.014	Present

[18] and the Fréjus experiment [19]. ^{16}O (target) result is deduced from the KAMIOKANDE water Cherenkov experiment [20].

V. REMARKS

The obtained limits in the present inclusive measurement are relevant to mode-independent nucleon decays (instabilities). The present values are comparable to the values deduced from inclusive geochemical methods [17]. The present limits are based on the on-line data, which are free from the cosmic-ray induced background in contrast to the geochemical method. It is noted here that the present limit can be applied for invisible modes such as $n \rightarrow 3\nu$, $nn \rightarrow 2\nu, \dots$, without being accompanied by charged particles. The obtained limits on dineutron decay are comparable to the limits on $nn \rightarrow \nu_e \bar{\nu}_e$ and $nn \rightarrow \nu_\mu \bar{\nu}_\mu$ decays measured by the exclusive measurement [19].

In short the present work gives for the first time the limits on mode-independent multinucleon decays, by looking for the possible x rays and γ rays associated with

radioactive residual nuclei produced by the nucleon decays. The limits on the mode independent single-nucleon decays were also obtained. The present limits are applied for the invisible decay modes of $n \rightarrow 3\nu$, $2n \rightarrow 2\nu$, $3n \rightarrow x\nu$, etc.

Note added in proof. The limits given in the text are obtained by assuming that all the decaying particles escape from the nucleus without internuclear collision as in case of neutrinos.

ACKNOWLEDGMENTS

The authors thank Professor E. Takasugi, Professor M. Fujiwara, Professor T. Kishimoto, and Dr. J. Tanaka for valuable discussions, and H. Kinoshita, the ELEGANTS group of Osaka University for the help during the run, and the Kamioka Mining and Smelting Co., Ltd., Mitsui Co., Ltd., and the ICRR group for their kind support at Kamioka. This work was supported by the Grant-in-Aid of Scientific Research and Ministry of Education, Science and Culture, Japan.

-
- [1] G. Feinberg and M. Goldhaber, Proc. Natl. Acad. Sci. U.S.A. **45**, 1301 (1959).
 - [2] P. Langacker, Phys. Rep. **72**, 185 (1981), and references therein.
 - [3] F. Reines and M. F. Crouch, Phys. Rev. Lett. **32**, 493 (1974).
 - [4] K. S. Hirata *et al.*, Phys. Lett. B **220**, 308 (1989).
 - [5] S. Seidel *et al.*, Phys. Rev. Lett. **61**, 2522 (1988).
 - [6] Fréjus Collaboration, Ch. Berger *et al.*, Nucl. Phys. **B313**, 509 (1989).
 - [7] R. Becker-Szendy, Phys. Rev. D **42**, 2974 (1990).
 - [8] H. Georgi and S. L. Glashow, Phys. Rev. Lett. **32**, 438 (1974); H. Georgi, H. R. Quinn, and S. Weinberg, *ibid.* **33**, 451 (1974).
 - [9] J. C. Pati and A. Salam, Phys. Rev. D **8**, 1240 (1973); **10**, 275 (1974); Phys. Rev. Lett. **31**, 661 (1973); R. N. Mohapatra and R. E. Marshak, *ibid.* **44**, 1316 (1980); H. Fritzsh and P. Minkowski, Ann. Phys. (N.Y.) **93**, 193 (1975).
 - [10] H. Ejiri, in *Proceedings of the International Seminar on the Frontier of Nuclear Spectroscopy*, Kyoto, 1992, edited by Y. Yoshizawa, H. Kusakari, and T. Otsuka (World Scientific, Singapore, 1993), p. 261; Phys. Rev. C **48**, 1442 (1993).
 - [11] H. Ejiri and H. Toki, Phys. Lett. B **306**, 218 (1993).
 - [12] H. Ejiri *et al.*, Nucl. Instrum. Methods **A302**, 304 (1991).
 - [13] H. Ejiri *et al.*, Phys. Lett. B **258**, 17 (1991).
 - [14] H. Ejiri *et al.*, Phys. Lett. B **282**, 281 (1992).
 - [15] A. Bohr and B. R. Mottelson, *Nuclear Structure* (Benjamin, New York, 1969).
 - [16] R. Brun *et al.*, GEANT3, CERN DD/EE/84-1 (1987).
 - [17] J. C. Evans, Jr. and R. I. Steinberg, Science **197**, 989 (1977).
 - [18] J. Learned, F. Reines, and A. Soni, Phys. Rev. Lett. **43**, 907 (1979).
 - [19] C. Berger *et al.*, Phys. Lett. B **269**, 227 (1991).
 - [20] Y. Suzuki *et al.*, Phys. Lett. B **311**, 357 (1993).